TDDFT study of excitation of water molecules with short laser pulses*

Wang Zhi-Ping(王志萍)†, Wu Ya-Min(吴亚敏), Zhang Xiu-Mei(张秀梅), and Lu Chao(鲁 超)

School of Science, Jiangnan University, Wuxi 214122, *China*

(Received 30 October 2012; revised manuscript received 22 November 2012)

We explore the excitation of water molecules subject to short and intense laser pulses in the frame of time-dependent density function theory (TDDFT) at the level of the time-dependent local-density approximation (TDLDA), applied to valence electrons, coupled non-adiabatically to molecular dynamics (MD) of ions. We first study the optical absorption spectra of the water molecule as an observable in the "linear" domain and results are in good agreement with experiments. We then explore the influence of the laser frequency on the excitation. It is found that when the laser frequency is off-resonant or highly above the resonant region, the excitations are weak whereas for the resonant frequency case, the ionization is enhanced and bond lengths are enlarged. Furthermore, a direct coupling of ions with the laser pulse with the off-resonant frequency is found when investigating the OH bond lengths. We finally study the effect of laser intensity on the excitation of H_2O and it is found that ionization increases when the laser intensity varies from low to high and we observe stable vibrations to Coulomb fragmentation when the ionization is up to typically two more charge units.

Keywords: time-dependent local-density approximation, ionization, optical absorption spectra

PACS: 33.20.–t, 31.15.E–, 34.50.Gb, 36.40.Vz **DOI:** 10.1088/1674-1056/22/7/073301

1. Introduction

Water has been one of the most explored substances because of its importance to all life and its complex properties.[1,2] Excitation of the water molecule with femtosecond laser pulses is an extremely versatile tool to trigger and to analyze a world of dynamical processes. These processes range from the simple optical response[3] to multiphoton ionization.[4] More recently, much effort has been devoted to the investigation of the coordination and electrostatic effects on the electronic and optical properties of water.[5–8] Excitation energies and vibrational frequencies of the water molecule have been studied theoretically applying the real-space pseudopotential calculations, as well as asymptotically corrected and hybrid functional in the framework of time-dependent DFT.[9,10] These studies obtained excitation energies in closer agreement with corresponding experiments. On the other hand, the modern lasers provide flexible and powerful pulses to study the photo-induced dynamics of molecules,[11] and there have been a number of investigations on the irradiation of neutral and charged water clusters[12–14] and other polyatomic molecules.[15,16] However, up to now, less effort has been devoted to exploring the irradiation of the water molecule subject to the laser field systematically. Our aim of this contribution is to present a first systematical exploration of the dynamics of the water molecule in the laser field using TDLDA-MD which has proven to be a robust model for non-linear dynamics in metal clusters and organic molecules.[17–19]

2. Theory and simulation details

The laser-induced electronic and ionic dynamics are explored by TDLDA-MD[17] where electrons are described by TDLDA,[20] and ions are described within standard molecular dynamics. There are six valence electrons and three ions in the water molecule. The total energy of H_2O is given by

$$\begin{aligned} E &= E_{\mathrm{k,e}}(\{\varphi_j\}) + E_{\mathrm{k,i}}(\{\dot{\boldsymbol{R}}_i\}) + E_{\mathrm{C}}(\rho) + E_{\mathrm{xc}}^{\mathrm{LDA}}(\rho^{\uparrow},\rho^{\downarrow}) \\ &\quad + E_{\mathrm{SIC}}(\{|\varphi_j|^2\}) + E_{\mathrm{p,i}}(\{\boldsymbol{R}_i\}) \\ &\quad + E_{\mathrm{PsP}}(\{\varphi_j\},\{\boldsymbol{R}_{\mathrm{I}}\}) + E_{\mathrm{ext}}, \end{aligned} \tag{1}$$

where $E_{\mathrm{k,e}}$, $E_{\mathrm{k,i}}$, E_{C}, and $E_{\mathrm{p,i}}$ are the kinetic energy and Coulomb potential of electrons and ions, respectively, $E_{\mathrm{xc}}^{\mathrm{LDA}}$ is the energy-density functional for electronic exchange, and the parameterization of Perdew and Wang[21] is applied. The E_{SIC} stands for the self-interaction correction term and an average-density self-interaction correction (ADSIC)[22] is used to put the single-particle energy at their correct values. The E_{ext} is the external potential, and $\varphi_j(\boldsymbol{r})$ denote single-particle orbitals satisfying the time-dependent Kohn–Sham (TDKS) equations.[23] The electron density is given by $\rho(\boldsymbol{r},t) = \sum_j |\varphi_j(\boldsymbol{r},t)|^2$. The electronic structure is governed by the Kohn–Sham Hamiltonian. The Hamiltonian equation of motion for ions is obtained by variation of $\boldsymbol{R}_i$ and $\boldsymbol{P}_i$. The interaction between ions and electrons (E_{PsP}) is described by means of a norm-conserving Goedecker-type pseudopotential,[24] including a local part and a non-local part. All of them employ Gaussians augmented by a polynomial. The ground state wavefunctions are determined by the damped gradient method.[17] The TDLDA equations are

*Project supported by the National Natural Science Foundation of China (Grant No. 61178032), the Fundamental Research Funds for the Central Universities of China (Grant No. 11A21), and the "Eleven Five" Planning Issues for Higher Education of Jiangsu Province, China (Grant No. JS053).

†Corresponding author. E-mail: zpwang03247@163.com

© 2013 Chinese Physical Society and IOP Publishing Ltd

solved numerically on a grid 3D coordinate space (cuboid box of size $64\times64\times64$) with a grid spacing of $0.412a_0$ and a constant time step $\Delta t = 0.0125$ a.u. For the nonlocal part contained in the Hamiltonian, it is dealt with in an additional propagator and treated with a third-order Taylor expansion of the exponential.[25] The absorbing boundary condition is employed to avoid periodic reflecting electrons.[26]

Ignoring the magnetic field component, the laser field is written as

$$V_{\rm las} = E_0 z f(t)\cos(\omega t), \tag{2}$$

where $E_0 \propto \sqrt{I}$ with I denoting the intensity, z is the dipole operator, $f(t)$ is the pulse profile in the form of $\cos^2(t)$, and ω is the laser frequency. The full width at half maximum (FWHM) is 20 fs.

The number of electrons in bound states $N(t)$ can be obtained by

$$N(t) = \int_V {\rm d}^3 r \rho(\boldsymbol{r},t), \tag{3}$$

where $\rho(\boldsymbol{r},t)$ denotes the electronic density within the finite volume V centered around the ionic background. Thus, the number of escaped electrons can be defined as $N_{\rm esc} = N(t=0) - \int_V {\rm d}^3 r \rho(\boldsymbol{r},t)$.

To calculate the optical response, our initial wave functions are perturbed from the static solutions φ_j by an external field which is turned on instantaneously at $t = 0$, adopting $V_{\rm ext} = k_0 r_\nu \delta(t)$ $(\nu = x,y,z)$ producing an initial state for the time evolution as

$$\varphi_j(\boldsymbol{r},0_+) = {\rm e}^{-{\rm i}k_0 r_\nu}\varphi_j(\boldsymbol{r}), \quad \nu = x,y,z. \tag{4}$$

The momentum k_0 is set to be small to ensure that the response is linear. The real-time evolution of the dipole moment can be obtained by $D_i(t) = \int {\rm d}^3 \boldsymbol{r} r_i \rho(\boldsymbol{r},t)$ $(i = x,y,z)$. Fourier transform the dipole momentum $\boldsymbol{D}(t)$ into the frequency domain and the optical absorption strength is the imaginary part of $\tilde{\boldsymbol{D}}(\omega)$.[25]

2.1. Results and discussion

2.1.1. Ground state and optical response

The water molecule is in the x–y plane. The oxygen ion is on the x axis and two hydrogen ions are symmetrical with respect to the y axis. Figure 1 exhibits the ground state of the ionic structure and the contour plot of the electronic density of H_2O. It is clear that the ions localize around the origin of the calculation box and electrons concentrate well around ions, which indicates that the computation space is large enough to launch the dynamic calculation.

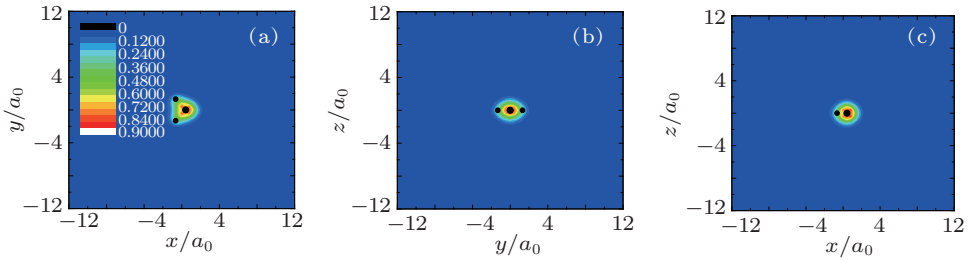


Fig. 1. (color online) The ground state of the ionic structure and the contour plots of the electronic density of H_2O in the (a) x–y plane, (b) y–z plane, and (c) x–z plane, respectively. Full black circles stand for oxygen and hydrogen ions.

The spectral distribution of optical absorption strength (optical response) provides key information on the coupling of a system to laser pulses. The initial response is mostly mediated by electrons. The optical response is related to eigenfrequencies of electronic excitations which exhibit well isolated peaks at frequencies below emission threshold and continuum above.

Figure 2 shows the optical absorption spectra of H_2O obtained by TDLDA. To compare with the experiment result, the results from Ref. [27] are exhibited. Comparing the two curves in Fig. 2, it is easy to find that the trends of curves are similar. Looking clearly at the black curves, one can find that the optical absorption spectra of H_2O exhibits typical structures with well-marked and isolated peaks. The lowest peak is located at 8.77 eV, which is consistent with 8.2 eV for liquid water and the experiment value 8.7 eV for ice (in its hexagonal, cubic, and amorphous phase).[27–30] The other typical peaks at 11.04, 12.72, and 15.23 eV also agree well with the optical spectrum of water surrounding the hydrate environment of crystalline ice,[7] which are 10.8, 12.7, and 14.2 eV, respectively.

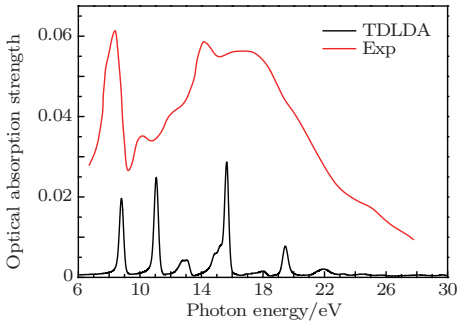


Fig. 2. (color online) The optical absorption strength of H_2O. The red line stands for the experiment results of the hexagonal ice from Ref. [27] and the black line represents the results obtained by TDLDA.

2.1.2. Dependence of the laser frequency

Now we consider the influence of laser frequency on irradiation dynamics of the water molecule. Figure 3 shows the irradiation of H_2O by lasers with polarization along the x axis, FWHM of 20 fs, and intensity of $I = 1 \times 10^{13}$ W/cm^2. Three laser frequencies are considered, which are $\omega = 0.68$ eV (out of the resonant region), $\omega = 13.6$ eV (in the resonant region with the nucleus (the rest energy hon), and $\omega = 136$ eV (high above the resonant region and ultra-violet (UV)). The parameters of lasers are shown in Fig. 3. In order to observe the dynamic motion of H_2O in the relaxation time, after the laser pulse is switched off at 40 fs, we track the calculation until 50 fs.

First, look at the left column in Fig. 3. It shows clearly the different responses of the dipole moment. For the case of $\omega = 0.68$ eV, the frequency is far below the resonant region such that one may speak of an adiabatic excitation. The result in Fig. 3(a) shows clearly that the amplitude of the dipole signal follows the laser field well during the pulse duration and keeps on oscillating gently in the relaxation time and the final $N_{\rm esc}$ is 0.005. This pattern is very similar to that found in the metal clusters when irradiated by an optical laser with frequency off the plasmon resonance.[31]

The resonant case in Fig. 3(b) exhibits a very different behavior. The dipole evolution shows a complex pattern. The onset still follows the laser amplitude. However, the resonant coupling results in the reduction of the dipole oscillations soon at around 17 fs. There is again a small and a large increase of the oscillations at around 21 fs and 32 fs because the charge system drives the next peak in the optical response into resonance with the laser. Because of the damping by ongoing electron ionization, the amplitude of dipole signal decays and the dipole signal continues to oscillate long after the laser pulse has died out and more ionization is observed ($N_{\rm esc} \approx 0.1$).

For the UV case in Fig. 3(c), we can see again an off-resonant process. The envelope of the dipole signal closely follows the laser amplitude and the signal basically disappears when the laser is switched off and the final ionization is 0.006. The suppression of ionization is due to the fact that the laser field oscillates so fast that a large fraction of electronic density is kicked back before it can gain substantial velocity to escape. This strong suppression of frequency is well accounted for in the Keldysh parameter describing an effective laser strength.[32] Furthermore, one can see some small and fast oscillations on top of the dipole profile resulting from the quiver motion of electrons.

The right column of Fig. 3 shows the time evolution of the bond lengths of OH bonds in H_2O. In order to see clearly the difference between three cases, the scale of the y axis takes the same value. First, one can see from Fig. 3(d) that OH bonds start to oscillate around the value of $1.7a_0$ at around 5 fs. The vibration amplitude increases gradually and attains a stable value at around 25 fs. The OH bonds keeps on oscillating stably long after the pulse is turned off.

The OH bonds in Fig. 3(e) exhibit a totally different pattern. The bond lengths start to increase slowly at around 10 fs which is 5 fs later than the electronic motion in Fig. 3(b). This indicates that the ions follow the electrons and electronic dynamics dominates in the resonance case. Finally, the OH bond lengths attain a new stable value of $1.705a_0$ at around 30 fs and continue to oscillate around this new value in the relaxation time. Thus, in the resonant case, the stable OH bond length is enlarged.

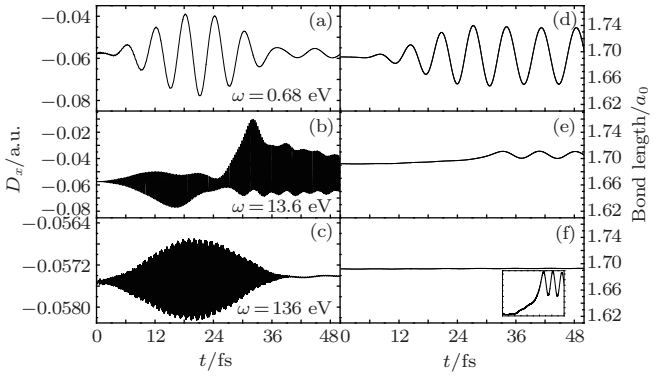


Fig. 3. The time evolutions of the dipole moment in x direction (left column), and bond lengths of OH bonds (right column).

For the UV case in Fig. 3(f), one can find that the lengths of OH bonds changes very little during the whole calculation time. The inset in Fig. 3(f) gives more clearly the image of evolution of lengths. One can find that OH bonds do oscillate as soon as the laser pulse acts on H_2O whereas the amplitude is so small that one could not even see that in Fig. 3(f). Moreover, comparing oscillation amplitudes in Figs. 3(d)–3(f), it is easy to find that the ions vibrate most strongly in the case of $\omega = 0.68$ eV. This aspect can be traced back to a direct coupling of the ions with the laser itself in the off-resonant cases.

2.1.3. Dependence of the laser intensity

In this section we consider the influence of laser intensity on irradiation dynamics of the water molecule. Figure 4 shows the result from excitation at $\omega = 13.6$ eV but with larger intensity. From Fig. 4(a) one can easily find that about three electrons out of the six electrons are emitted in a comparatively short time (from 5 fs to 35 fs) resulting in the molecule being grossly Coulomb unstable. Correspondingly, as shown in Figs. 4(b) and 4(c), ionic coordinates in x and y directions show clearly the pattern of a straight Coulomb explosion of H_2O in the x–y plane.

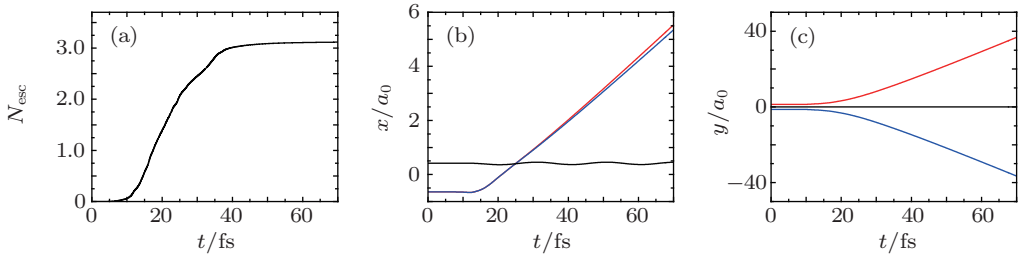


Fig. 4. (color online) Irradiation of H_2O by a laser with polarization along the x axis, FWHM of 20 fs, intensity of $I = 5 \times 10^{14}$ W/cm^2 and $\omega = 13.6$ eV. (a) The time evolution of N_{esc}. (b) The time evolution of ionic x coordinates. (c) The time evolution of ionic y coordinates. The black line is for the oxygen ion. The red and blue lines are related to two hydrogen ions, respectively.

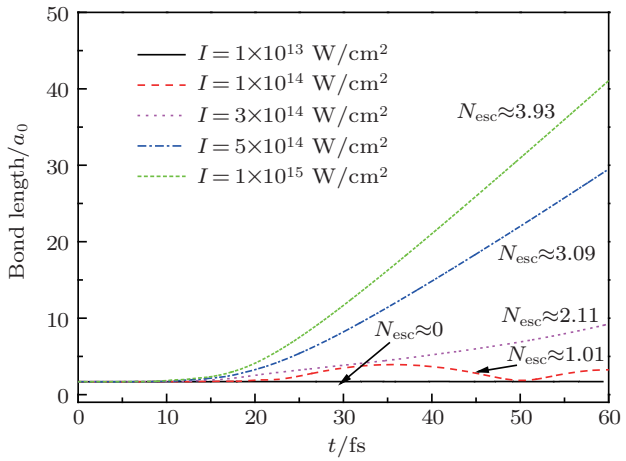


Fig. 5. (color online) Time evolution of bond lengths of OH bonds in H_2O. The laser polarization is along the x axis, FWHM of 20 fs, and $\omega = 13.6$ eV. Four different intensities are considered. The number of emitted electrons N_{esc} is also indicated for each case.

To see clearly how the bond lengths of H_2O depend on the laser intensity, figure 5 represents five cases with different laser intensities. The influence of laser intensity on the ionic response is obvious. First, from the value of N_{esc} in Fig. 5, one can observe increasing ionization with increasing intensity. Second, for two low intensity cases, on the time scales computed here, OH bonds oscillate gently and the oscillation amplitude increases because of the larger field strength (the black solid and red dashed lines in Fig. 5) and H_2O seems to resist fragmentation and keep its vibrational response. Furthermore, when the net ionization is larger than two, the general vibrational style changes. With increasing intensity, the OH bond length increases directly (reflecting the fragmentation of H_2O) during the computation time and the slope of OH bond length as a function of time increases (the magenta dotted line, the blue dashed-dotted line and the green short dash line in Fig. 5). To sum up, we thus observe a substantial vibration response with increasing laser intensity.

Figure 6 shows the number of escaped electrons N_{esc} at 40 fs (as soon as the laser pulse switched off) versus intensity I for frequencies of 6.8, 13.6, and 20.4 eV, respectively. It is easy to see in Fig. 6 that electron emission shows a steady slope in the regime of low intensity, off as well as on resonance, resulting from the ionization of the easily accessible valence electrons. This accords well with the multi-photon perturbation theory in the perturbative regime of low electron yield.[33] With increasing intensity, the deviations from the linear behavior occur. Furthermore, it can be found that the relative positions of curves are mainly determined by the relation of laser frequency to resonant frequencies (as discussed in Fig. 2): the farther the laser frequency from the resonant region, the higher the intensity needed to initiate ionization.

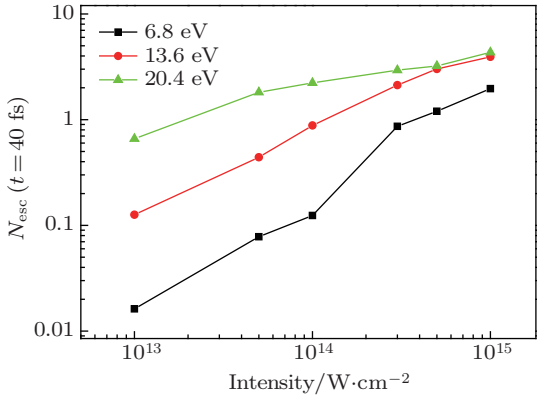


Fig. 6. (color online) Number of emitted electrons N_{esc} versus laser intensity for various frequencies as indicated.

3. Conclusion

In this paper we have explored the dynamical response of H_2O to a short and intense laser pulse with the help of TDLDA-MD approach which has proven to be a robust model for non-linear dynamics in metal clusters and organic molecules. We first briefly discussed the "optical" response as an observable in the "linear" domain which serves as a guideline for understanding the behavior of the system under stronger irradiations. We then demonstrated the versatility of a laser excitation when playing with its frequency. When the laser frequency is off-resonant or highly above the resonant region, the ionization is rather small and the dipole signal behaves as a classical oscillator in both cases. In contrast, for the resonant case, there is a substantial electronic emission and a strong damping of the dipole moments. The investigation of the OH bond lengths reveals that, in the off-resonant case, ions couple with the laser field directly, i.e., the electrons follow the ions, whereas in the resonant case, the ions follow the

electrons and OH bond lengths are enlarged. We have also studied the effect of laser intensity on the excitation of H_2O. Ionization increases when the laser intensity varies from low to high and we observe stable vibrations to Coulomb fragmentation when the ionization is up to typically two more charge units.

References

[1] Ludwig R 2001 *Angew. Chem. Int. Ed.* **40** 1808

[2] Bukowski R, Szalewicz K, Groenenboom G C and Avoird Ad van der 2007 *Science* **315** 1249

[3] Kreibig U and Vollmer M 1993 *Optical Properties of Metal Clusters* (Berlin: Springer Series in Materials Science)

[4] Faisal 1987 *Theory of Multiphoton Processes* (New York: Plenum Press)

[5] Garbuio V, Cascella M, Reining L, Del S R and Pulci O 2006 *Phys. Rev. Lett.* **97** 137402

[6] Hahn P H, Schmidt W G, Seino K, Preuss M, Bechstedt F and Bernholc J 2005 *Phys. Rev. Lett.* **94** 037404

[7] Hermann A, Schmidt W G and Schwerdtfeger P 2008 *Phys. Rev. Lett.* **100** 207403

[8] Garbuio V, Cascella M and Pulci O 2009 *J. Phys.: Condens. Matter* **21** 033101

[9] del Puerto M L, Tiago M L, Vasiliev I and Chelikowsky J R 2005 *Phys. Rev. A* **72** 052504

[10] Cai Z, Tozer D J and Reimers J R 2000 *J. Chem. Phys.* **113** 7084

[11] Chen D Y, Zhang S and Xia Y Q 2009 *Chin. Phys. B* **18** 3073

[12] Sternovsky Z, Horányi M and Robertson S 2001 *Phys. Rev. A* **64** 023203

[13] Lammich L, Domesle C, Jordon-Thaden B, Förstel M, Arion T, Lischke T, Heber O, Klumpp S, Martins M, Guerassimova N, Treusch R, Ullrich J, Hergenhahn U, Pedersen H B and Wolf A 2010 *Phys. Rev. Lett.* **105** 253003

[14] Kumarappan V, Krishnamurthy M and Mathur D 2003 *Phys. Rev. A* **67** 063207

[15] Xiong D L, Wang M S, Yang C L, Tong X D and Ma N 2010 *Chin. Phys. B* **19** 103303

[16] Yan B and Pan S F 2008 *Chin. Phys. B* **17** 1501

[17] Calvayrac F, Reinhard P G, Suraud E and Ullrich C A 2000 *Phys. Rep.* **337** 493

[18] Wang Z P, Dinh P M, Reinhard P G, Suraud E and Zhang F S 2011 *Inter. J. Quanm. Chem.* **111** 480

[19] Fennel Th, Meiwes-Broer K H, Tiggesbäumker J, Reinhard P G, Dinh P M and Suraud E 2010 *Rev. Mod. Phys.* **82** 1793

[20] Dreizler R M and Gross E K U 1990 *Density Functional Theory: An Approach to the Quantum Many-Body Problem* (Berlin: Springer)

[21] Perdew J P and Wang Y 1992 *Phys. Rev. B* **45** 13244

[22] Legrand C, Suraud E and Reinhard P G 2002 *J. Phys. B* **35** 1115

[23] Gross E K U and Kohn W 1990 *Adv. Quant. Chem.* **21** 255

[24] Goedecker S, Teter M and Hutter J 1996 *Phys. Rev. B* **54** 1703

[25] Calvayrac F, Reinhard P G and Suraud E 1997 *Ann. Phys.* **255** 125

[26] Ullrich C A 2000 *J. Mol. Struct.* **501** 315

[27] Kobayashi K 1983 *J. Phys. Chem.* **87** 4317

[28] Kerr G D, Hamm R N, Williams M W, Birkhoff R D and Painter L R 1972 *Phys. Rev. A* **5** 2523

[29] Heller J M, Hamm R N, Birkhoff R D and Painter L R 1974 *J. Chem. Phys.* **60** 3483

[30] Hayashi H, Watnanbe N, Udagawa Y and Kao C C 2000 *Proc. Natl. Acad. Sci.* **97** 6264

[31] Ullrich C A, Reinhard P G and Suraud E 1997 *J. Phys. B* **30** 5043

[32] Keldysh L V 1965 *Sov. Phys. JETP* **20** 1307

[33] Gavrila M 1992 *Atoms in Intense Laser Fields* (San Diego: Academic Press)